Available online at www.sciencedirect.com
SCIENCE DIRECT®
Journal of Chromatography A, 1053 (2004) 291–297
JOURNAL OF CHROMATOGRAPHY A
www.elsevier.com/locate/chroma

Effect of solvent composition on signal intensity in liquid chromatography–matrix-assisted laser desorption ionization experiments

Stephen J. Hattan*, Jason Marchese, Michael Albertinetti, Srinivasan Krishnan, Nikita Khainovski, Peter Juhasz

Applied Biosystems, Discovery Proteomics and Small Molecule Research Center, 500 Old Connecticut Path, Framingham, MA 01701, USA

Available online 17 September 2004

Abstract

The use of reversed phase liquid chromatography for the preparation of complex peptide mixtures for analysis by matrix assisted laser desorption ionization mass spectrometry has led to the observation of the critical importance of the matrix/analyte formulation in regards to the percent organic solvent in the mixture. This paper outlines the study using liquid chromatography to systematically vary the acetonitrile concentration in the formulation used for MALDI spot preparation to examine the impact the parameter has on analyte signal intensity. The results show that for five of six peptides tested across a wide mass range a formulation of approximately 75% acetonitrile is optimal for average MALDI signal intensity as determined on both time-of-flight and quadropole mass spectrometers. Examination of the individual spots shows that the organic solvent content in formulation significantly affects parameters such as crystal density and morphology.

Keywords: Matrix preparation; Matrix-assisted laser desorption ionization; Signal intensity

1. Introduction

Since its inception in the 1980s matrix-assisted laser desorption ionization–time of flight (MALDI–TOF) [1] mass spectrometry has been used to accurately determine the masses of proteins [2], peptides [3–5], nucleic acids [6,7] and other biologically relevant compounds. A key requirement for successful MALDI analyses is the incorporation of the analyte into a crystalline matrix [8,9]. Most MALDI matrices are UV absorbing organic compounds with carboxylic and/or phenol groups [10–12]. Typical sample preparation procedures involve the mixing of analyte and matrix in a solution composed of water and a miscible organic solvent (acetonitrile, methanol, propanol, etc.). The sample is placed on a suitable target and allowed to dry. Under optimum conditions, the analyte will adsorb to the faces of the growing matrix crystal, eventually producing analyte-doped crystals on the target [13,14]. The success of this process depends on physicochemical variables characteristic of the analyte–matrix interaction and, as this study will show, on the composition of the dilution solvent.

For the analysis a complex peptide samples, liquid chromatography is routinely used to separate or simplify the sample material prior to mass spectrometry [15–18]. MALDI can be hyphenated with narrow-bore and capillary chromatography off-line so the eluting sample may be immediately co-mixed with the matrix solution and spotted in discrete time intervals onto the MALDI target in an automated manner [19–21]. In this way the chromatographic resolution is preserved on the sample plate and can be analyzed in MS and MS/MS modes in a manner best suited for the experiment [22]. Reversed-phase chromatography is often the chromatographic mode of choice due to its resolution, peak capacity, and compatibility with “mass spectrometry friendly” sol-

* Corresponding author. Tel.: +1 508 383 7635; fax: +1 508 383 7893.
E-mail address: hattansn@appliedbiosystems.com (S.J. Hattan).

0021-9673/$ – see front matter © 2004 Published by Elsevier B.V.
doi:10.1016/j.chroma.2004.07.094

Table 1
HPLC gradient used in the experiment

Time (mm:ss)	Flow (μL/min)	Value (%A)	Value (%B)
00:00	0.800	100	0
20:00	0.800	0	100
22:00	0.800	0	100
42:00	0.800	100	0
55:00	0.800	100	0

Solvent A: 2% ACN, 0.1% TFA; solvent B: 90% ACN, 0.1% TFA.

vents. One aspect of the LC–MALDI coupling to be aware of is the changing solvent composition of the effluent over the course of the LC gradient. The results of this change can be significant as the solubility and crystallization rate of the matrix depends greatly on the aqueous/organic ratio.

Present study will show that the composition of the dilution solvent has great influence on the size, distribution and morphology of the matrix crystals that translates into significant changes in the intensity of the MS signal. Previous investigations on MALDI sample preparation have demonstrated the influence of the solvent composition on the MS signal [23,24]. Studies have also been performed that focus on the optimum analyte/matrix ratio [25] sample drying time [23,26,27], optimum pH [23,28] optimum desorption laser fluence and pulse duration [29,30]. While these studies have provided insight into the processes involved in analyte–matrix co-crystallization and useful suggestions for sample preparation to improve data quality, a systematic investigation of the effect of solvent composition in HPLC–MALDI has not been reported.

In order to model the effects of the solvent composition on MALDI MS signal in HPLC–MALDI experiments, a gradient of HPLC solvents was generated and was co-mixed with matrix solution containing a mixture of standard peptides. Selecting a "saw tooth" shape for the gradient, the time-course of the peptide signal intensities was recorded. After making the necessary corrections for the delays for the HPLC lines, the relative intensities of the peptide signals could be represented against the solvent composition. Experiments have been made on both an axial TOF and an orthogonal TOF instrument in order to distinguish generic trends from instrument specific ones. The investigations were limited to peptides and α-cyano-4-hydroxycinnamic acid matrix (ACHCA) hence the findings cannot be generalized to other matrix/analyte systems. Still, the methodology can easily be applied to any matrix–analyte–solvent combination that would be used in an LC–MALDI workflow.

2. Materials and methods

2.1. Liquid chromatography and MALDI target preparation

Off-line coupling of nano-HPLC and MALDI was accomplished using an Ultimate Chromatography system equipped with a Probot fraction collector for MALDI spotting (both from Dionex-LC Packings, Hercules, CA, USA). A "saw tooth" gradient was generated to ramp up and down the organic content of the HPLC solvent mixture as outlined in Table 1. Mobile phase A consisted of 2% acetonitrile (ACN), 0.1% trifluoroacetic acid (TFA) and mobile phase B consisted of 90% ACN, 0.1% TFA. The LC effluent was mixed with the matrix solution using the built-in syringe pump of the Probot and a 25 nL mixing tee (Upchurch, WA, USA). Matrix concentrations of 10, 7.5 and 3 mg/mL α-cyano-4-hydroxycinnamic acid dissolved in 75:25 ACN–water containing 2% (w/w) dibasic ammonium-citrate were analyzed. Matrix solutions were spiked with a mixture of peptide standards listed in Table 2. The LC flow rate was set at 800 nL/min and the LC effluent and matrix were mixed in a 1:2 (v/v) ratio throughout the course of the gradient. The standard mixture of peptides used in the experiment were those contained in the Applied Biosystems 4700 Proteomics Analyzer mass standards kit. The lyophilized peptides were dissolved in 100 μL of 30% ACN, 0.1% TFA as described in the standard kit. This working stock solution was further diluted 200-fold with the matrix solution to give the final concentrations listed in Table 2.

Fraction collection onto the MALDI plate took place at 10-s intervals generating a 16 × 16 array of sample spots and MS analyses was performed on all spots.

2.2. Mass spectrometry

Mass spectrometric analysis was performed on an AB4700 Proteomics Analyzer (Applied Biosystems, Framingham, MA, USA) and on an oMALDI QSTAR® XL (MDS SCIEX, Concord, Ontario, Canada). For the 4700, MS mode acquisitions consisted of 2000 laser shots averaged over 50 sample

Table 2
Mass and concentration information for the peptides used the study

Peptide	$(M + nH)n^+$ monoisotopic (Da)	Concentration (fmol/μL) in matrix	Amount (fmol) on target	Matrix/analyte molar ratio on target
des-Arg^1-bradykinin	904.4681	83	25	445, 868
Angiotensin 1	1296.6853	167	51	218, 563
Glu^1-fibrinopeptide B	1570.6774	108	33	337, 779
ACTH (1–17)	2090.0067	167	51	218, 563
ACTH (18–39)	2465.1989	125	38	293, 334
ACTH (7–38)	3657.9294	250	76	146, 667

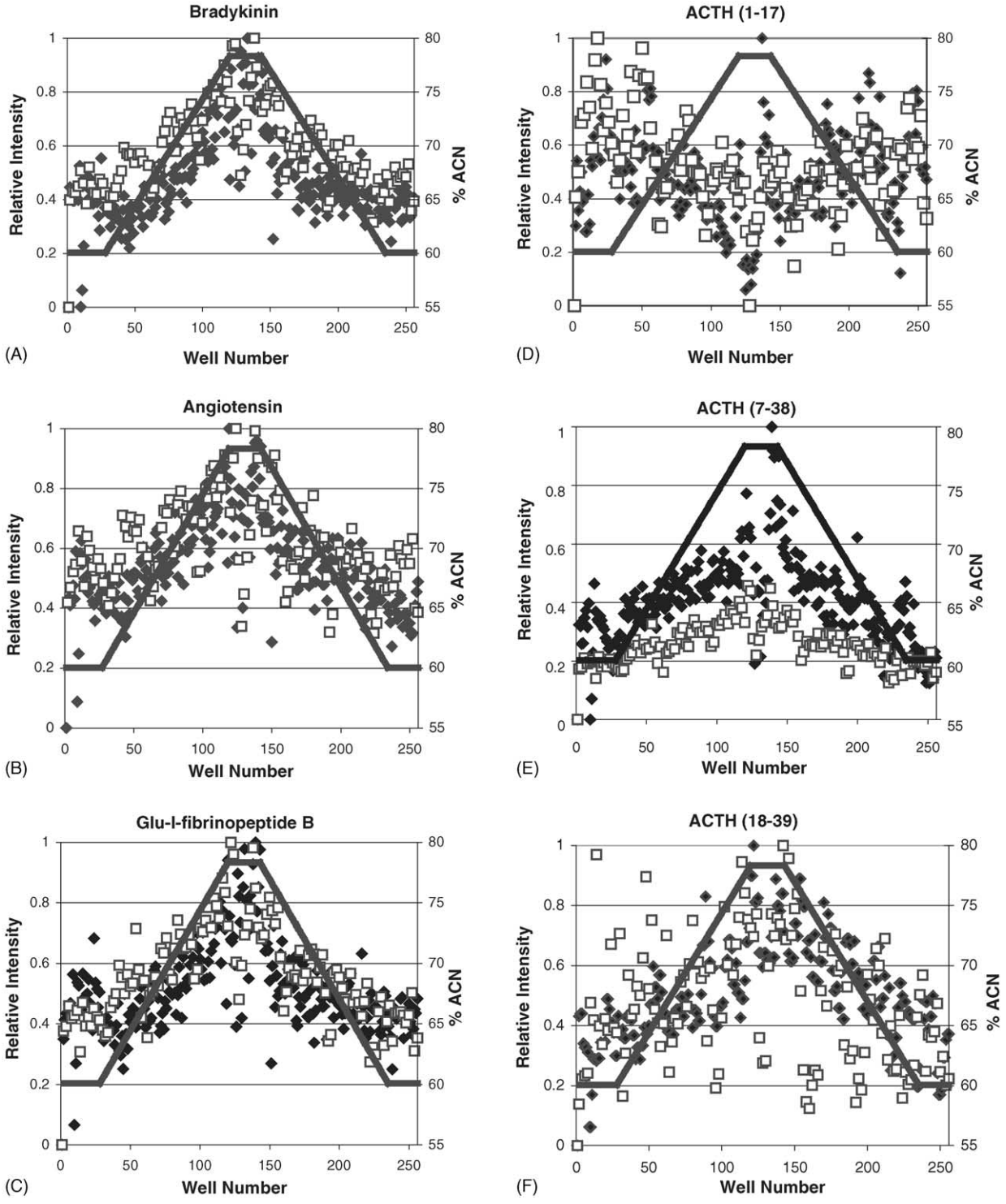

Fig. 1. Signal intensity (left axis) and %ACN (right axis) plotted against well number for the peptides spiked into the matrix: (A) bradykinin, (B) angiotensin, (C) Glu-fibrinopeptide B, (D) ACTH (1–17), (E) ACTH (18–39), (F) ACTH (7–38). In each plot (♦) = 4700 data and (□) = oMALDI Qstar data. The solid black trace outlines the ACN gradient.

positions ("search pattern positions") in order to minimize random signal variations. The signal intensity for the peptides the was determined by integration of the area under the peaks of the peptide isotope cluster and plotted as "cluster area." The QSTAR® XL hybrid system was fitted with an oMALDI™ 2 ion source. MS spectrum was acquired on each well using a Nitrogen laser (337 nm wavelength) at 20 Hz frequency and an output of 10 μJ. Each MS spectrum was an accumulation of ten 4 s scans in the mass range 900–4000 Da. Data on the 256 wells was acquired in automation using

the Analyst® QS and oMALDI™ Server software in batch mode.

2.3. Microscopy

Scanning electron microscope images were taken on a TOPCON SM-510 SEM (Topcon Corp., Tokyo, Japan) running with a Tungsten filament. Operating conditions were set to an accelerating voltage of 20 KV and a working distance of 15 mm. The sample plate was sputter coated with approximately 100–150 Å of gold using a Denton Vacuum Desk 2 cold sputter unit (Denton Vacuum, Moorestown, NJ).

Spot diameters were measured using an Olympus SZX12 light optical microscope (Olympus Optical Co. LTD, Tokyo Japan) equipped with a Micro Digital Read Out measurement system (Sempex Corp., Campbell, CA).

An in-house developed program, Crystal Distribution, was used to estimate the area within the spot that was composed of matrix crystals. The program acts by converting black and white images of MALDI spots to binary images based on the threshold value. An adjustable grayscale (0–255) is used to set the threshold. Any pixel value above the threshold is converted to white (1 value) and any pixel value below the threshold is converted to black (0 value). The threshold was adjusted manually so the crystals appeared white against a black background. Percent area calculation was performed over a user-defined region of interest (ROI). The program summed the pixel values in the ROI and divided by the total number of pixels to obtain the percentage of crystal coverage.

3. Results

Fig. 1A–F shows the signal intensity and the percentage of ACN in each MALDI fraction plotted against well number for the peptides spiked into the 7.5 mg/mL matrix as analyzed by the both AB4700 and the QSTAR®. Vertical scales of these charts are normalized to the intensity of the highest data point. As the plots clearly show, there is a strong relationship between signal intensity and ACN content of the deposition solvent. For each peptide except ACTH (1–17), the signal intensity increases as the ACN content increases and appears to reaches an optimum signal in the 73–78% ACN range depending on the peptide. Interestingly, as the ACN concentration plateaus at 78%, there is a noticeable decrease in signal intensity of the raw data for several of the peptides. Again, as the ACN content in the diluent drops along the downward slope of the gradient, the mass spectrometric signal reaches an optimum level of intensity between ∼73 and 78% ACN. Beyond this point it declines along with the ACN concentration. Signal intensity measurements using formulations with ACN concentrations of >78% were preformed for these same peptides on the 4700 (data not shown) and demonstrated the optimum value of between ∼73 and 78% as shown in the Fig. 1 data. This relationship between the MS signal intensity and solvent ACN concentration seems is consist regardless of peptide mass. However, the magnitude of the effect appears to be peptide dependent. The peptide ACTH (7–38) (3657.93 Da) undergoes a 4-fold signal increase while the other peptides in the mixture show an approximate 2- to 3-fold increase except ACTH (11–17). It should be noted the solvent conditions shown in Fig. 1 were chosen to be in the vicinity of optimal signal intensity. A broader variation in organic content has a more dramatic effect on analyte signal intensity. ACTH (1–17) showed the weakest response to the changing ACN conditions of the solvent; showing only an ∼2 fold sig-

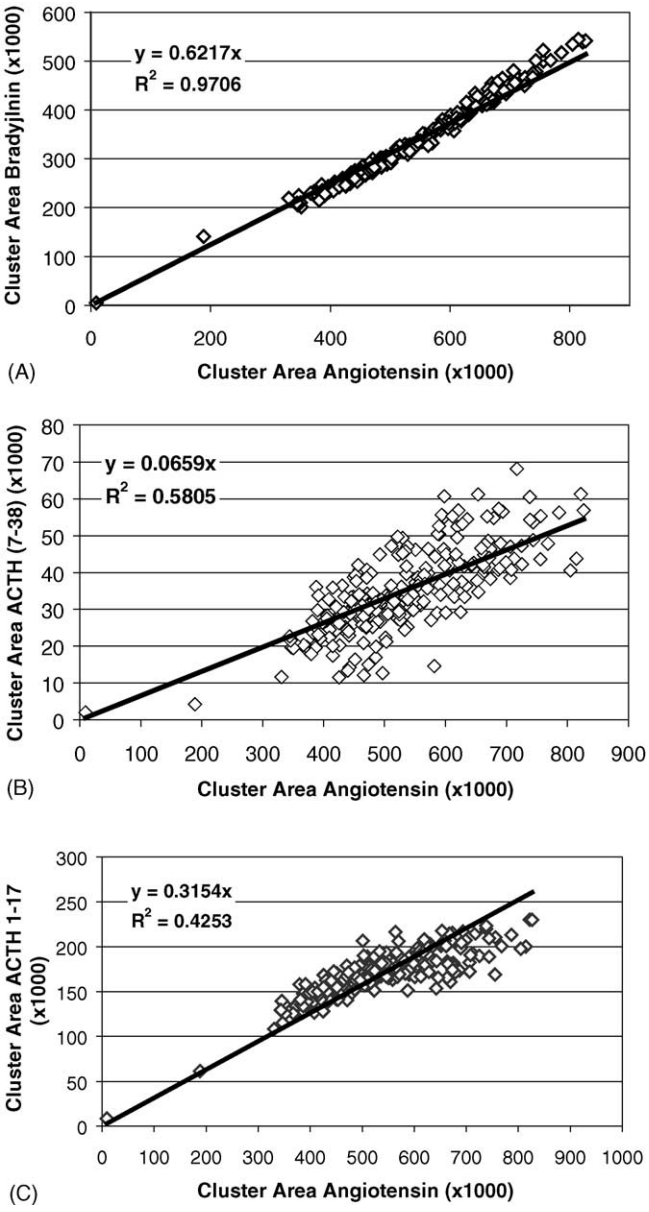

Fig. 2. (A) Plot of the signal intensity for angiotensin and bradykinin showing good correlation in the response of the two peptides. (B) Plot of the signal intensity of angiotensin and ACTH (7–39) and (C) plot of the signal intensity of angiotensin and ACTH (1–17), showing relatively poor correlation between the behavior of the peptides.

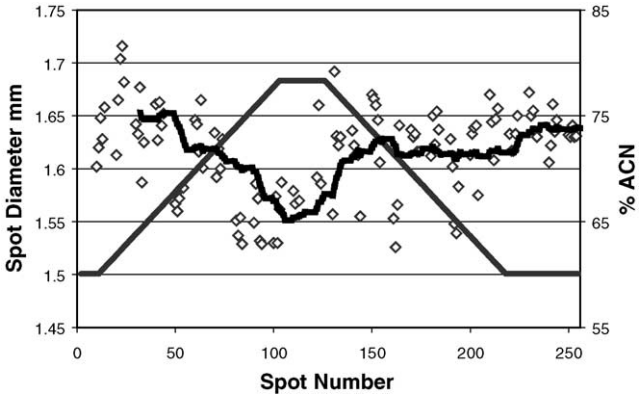

Fig. 3. Spot number plotted as a function of spot diameter and %ACN. The plot shows an inverse correlation between %ACN and spot size. The trendline through the raw data shows the move average across each row of spots (16 spots/row).

nal increase on going from 50 to 70% ACN (data not shown); however, the ACTH (1–17) plot in Fig. 1 clear demonstrates the decrease in signal that occurs as the ACN rises to 78%.

Fig. 2 shows scatter plots comparing the signal intensity for data collected on the 4700 Proteomics Analyzer for different peptides as a function of well number. Fig. 2A clearly shows that whatever influence the diluent solvent has on the interaction between the analyte and matrix it appears to affect the peptides in a similar manner. The Fig. 2A plot reveals a strong correlation (R^2 = 0.97) between in the signal intensity of angiotensin and bradykinin in a well-to-well comparison. Fig. 2B and C show similar plots for angiotensin plotted against ACTH (7–38) and ACTH (1–17) respectively. Although the trend is the same, the correlation between these later peptides is not as good (R^2 = 0.58 and R^2 = 0.42). It should also be noted that the relationship between angiotensin and ACTH (1–17) does not appear to be linear.

All acquisitions were performed in automated fashion using a random search pattern of 50 positions across the surface of the spot to the accumulation of 2000 laser shots (40 shots/per position) and manual searching for specific locations of elevated analyte concentration was not performed. The automated mode of acquisition coupled with the inherent in-homogeneity of crystallization and analyte distribution within a given spot leads to scatter in the data. However, mul-

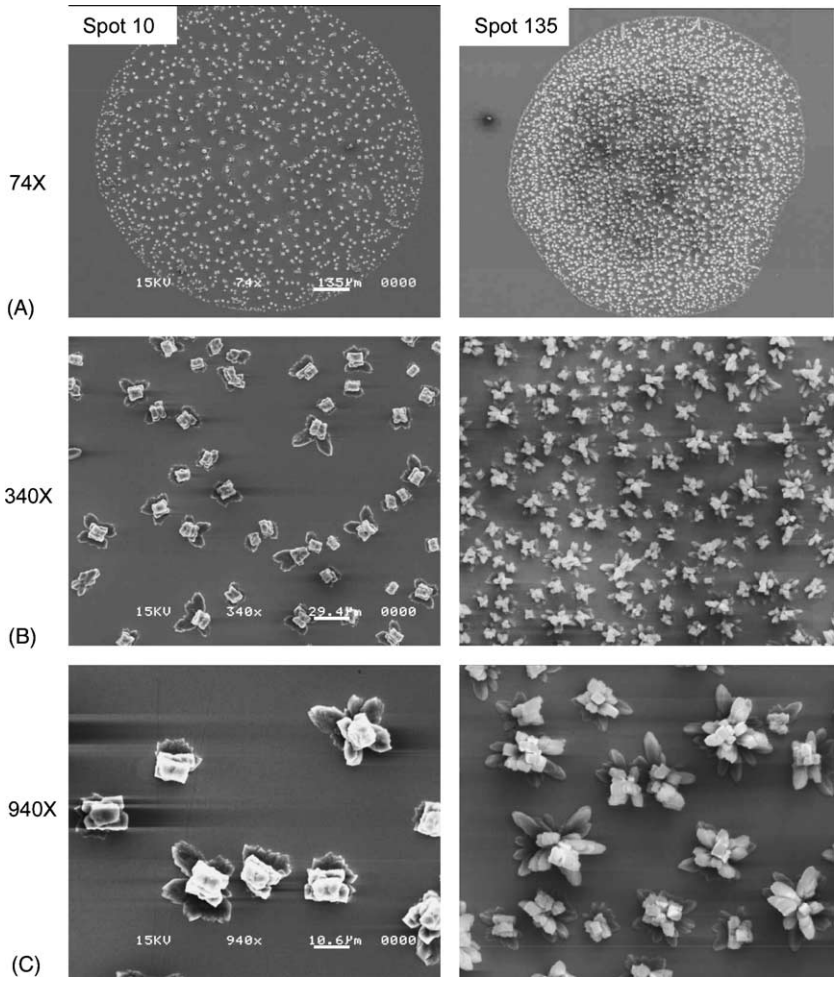

Fig. 4. SEM images comparing crystal morphology of spot 10 (50% ACN) and spot 135 (75% ACN) at (A) 74× (B) 340× and (C) 940×.

Table 3
Estimates of the density of matrix crystals in different regions of the ACN gradient

Spot range measured	Average %ACN	Average crystal density on spot	Standard deviation	*n*
19–26	62.32	12.64	1.63	4
70–77	72.53	17.68	3.63	4
135–141	75.95	20.09	3.17	4
180–186	67.04	16.27	2.37	4

tiple experiments performed using different ACN gradients, different analyte concentrations and different matrix concentrations all produced the same data trend. On average, spots prepared with a solvent formulation solvent in the vicinity of 75% ACN (with the remaining solution being composed of H_2O) and 0.1% TFA produces the maximum MS sensitivity for peptides across a wide mass range.

Fig. 3 shows an overlay plot of spot diameter and %ACN as measured for the odd numbered spots across the run. The plot shows that as the %ACN increases spot size tends to decrease. A moving average trend-line taken across each row of spots is superimposed on the raw data and shows that there is a approximate decrease in spot diameter from 1.65 to 1.55 mm on going from 50 to 78% ACN in the diluent solution. This decrease in spot diameter equals a 12% decrease in spot size based on an area calculation.

Fig. 4 shows three sets SEM images of two different spots. One spot contains a low ACN concentration (spot 10: ∼50% ACN) the other spot is located at the optimum ACN concentration (spot 135: ∼75% ACN). In addition to density of the crystals increasing as the ACN concentration increases, the images in Fig. 4 clearly show that the morphology of the crystals that form from spots containing different amount of ACN show distinct differences. Fig. 4 shows images at 70× (set A), 340× (set B) and 940× (set C). Looking at the individual crystals it is seen that the general geometry of the crystals changes as a result of solvent composition out of which they form. Crystals forming from a relatively low composition of organic solvent look more cubical as compared to the clusters of elongated shards that form out of a solvent with a high organic composition. The finds displayed in Fig. 4 prompted a measurement of the crystal density.

Table 3 shows the average density of the matrix crystals taken from different regions across the ACN gradient. The estimates were made using Labview software to estimate the contrast in images of the spot obtained on a scanning electron microscope. Four spots were imaged in each region and the average density of the matrix crystals and standard deviation of the measurement are shown. The data in Table 3 show the trend of an increase in density of the matrix crystals as the ACN concentration increases.

4. Conclusion

Sensitivity improvements by optimizing sample preparation play an important role in extending the scope of applications of MALDI mass spectrometry. This study offers a simple recommendation on how to optimize the matrix formulation in HPLC–MALDI MS experiments. It was shown that a solvent composed of approximately 75% ACN, 25% H_2O and 0.1% TFA produces the maximum MS sensitivity for peptides across a wide mass range. This finding can be utilized with dried droplet sample preparation and HPLC–MALDI off-line coupling as well. In the latter case the matrix solution that is co-deposited with the HPLC effluent onto the MALDI plate can be formulated so the final solvent composition on the plate as mixed from the HPLC effluent and the matrix solution is (symmetric) around the ∼75% ACN optimum. For instance, 80–85% ACN content of the matrix solution with 2–3:1 matrix solution-to-HPLC elution ratio would provide these conditions. These findings could be verified on multiple instrument platforms indicating a mechanism that is not dependent on the type of mass analyzer or on the pressure in the ion source. The data presented here-in are at a matrix concentration of 7.5 mg/mL ACHCA; however, experiments run at matrix concentrations of 10 and 3 mg/mL showed the same results.

A correlation between the signal intensity and the crystal distribution and size has been established. The variation of MS intensities with the crystal distribution is very likely the reason for our observations. The exact mechanism responsible for the intensity variations cannot be determined from these experiments. One can speculate though that the increased surface of a finer crystal distribution is beneficial for the MS signal intensity of peptides desorbed from ACHCA matrix. These is results do not necessarily generalize to other analyte/matrix combinations but the presented methodology can be applied easily to a wider variety of samples and matrices.

References

[1] M. Karas, F. Hillenkamp, Anal. Chem. 60 (1988) 2299.
[2] M. Lin, J.M. Campbell, D.R. Mueller, U. Wirth, Rapid Commun Mass Spectrom. 17 (2003) 1809.
[3] E.J. Takach, W.M. Hines, D.H. Patterson, P. Juhasz, A.M. Falick, M.L. Vestal, S.A. Martin, J. Protein Chem. 16 (1997) 363.
[4] R. Edmonson, D. Russell, J. Am. Soc. Mass Spectrom. 7 (1996) 995.
[5] O. Vorm, M. Mann, J. Am. Soc. Mass Spectrom. 5 (1994) 955.
[6] M.T. Roskey, P. Juhasz, I.P. Smirnov, E.J. Takach, S.A. Martin, L.A. Haff, Proc. Natl. Acad. Sci. U.S.A. 93 (1996) 4724.
[7] Y. Dai, R. Whittal, L. Li, S. Weinberger, Rapid Commun. Mass Spectrom. 10 (1996) 1792.
[8] F. Hillenkamp, M. Karas, R.C. Beavis, B.T. Chait, Anal. Chem. 63 (1991) 1193A.
[9] P. Juhasz, I.A. Papayannopoulos, C. Zeng, V. Papov, K. Biemann, Proceedings of the 40th Annual ASMS Conference on Mass Spectrometry and Allied Topics, Washington, DC, 1994, p. 1913.
[10] R.C. Beavis, T. Chaudhary, B.T. Chait, Org. Mass Spectrom. 27 (1992) 156.
[11] K. Strupat, M. Karas, F. Hillenkamp, Int. J. Mass Spectrom. Ion. Proc. 111 (1991) 89.

[12] J. Bai, X. Liang, Y.H. Liu, Y. Zhu, D.M. Lubman, Rapid Commun. Mass Spectrom. 10 (1996) 839.
[13] V. Horneffer, A. Forsmann, K. Strupat, F. Hillenkamp, U. Kubitscheck, Anal. Chem. 73 (2001) 1016.
[14] Y. Dai, R. Whittal, L. Li, Anal. Chem. 68 (1996) 2494.
[15] J. Malmstrom, K. Larsen, L. Malmstrom, E. Tufvesson, K. Parker, J. Marchese, B. Williamson, D.H. Patterson, S.A. Martin, P. Juhasz, G. Westergren-Thorsson, G. Marko-Varga, Electrophoresis 24 (2003) 3806.
[16] T. Rejtar, P. Hu, P. Juhasz, J.M. Campbell, M.L. Vestal, J. Preisler, B.L. Karger, J. Proteome Res. 1 (2002) 171.
[17] T. Miliotis, S. Kjellstrom, J. Nilsson, T. Laurell, L.-E. Edholm, G. Marko-Varga, Rapid Commun. Mass Spectrom. 35 (2000) 369.
[18] Y. Shen, R.D. Smith, Electrophoresis 23 (2002) 3106.
[19] T. Miliotis, S.O. Kjellstrom, P. Onnerfjord, J. Nilsson, T. Laurell, L.-E. Edholm, G. Marko-Varga, J. Chromatogr. A 886 (2000) 99.
[20] J. Preisler, P. Hu, T. Rejtar, E. Moskovets, B.L. Karger, Anal. Chem. 74 (2002) 17.
[21] M. Quadroni, P. James, Electrophoresis 20 (1999) 664.
[22] A. Graber, P. Juhasz, N. Khainovski, K.C. Parker, D.H. Patterson, S.A. Martin, J. Proteome Res. 4 (2004) 474.
[23] S.L. Cohen, B.T. Chait, Anal. Chem. 68 (1996) 31.
[24] K. Bornsen, M.A. Gass, G.J.M. Bruin, J.H.M. von Adrichem, M.C. Biro, G.M. Kresbach, M. Ehrat, Rapid Commun. Mass Spectrom. 11 (1997) 603.
[25] J. Yao, J.R. Scott, M.K. Young, C.L. Wilkins, J. Am. Soc. Mass Spectrom. 8 (1998) 805.
[26] F. Xiang, R.C. Beavis, Org. Mass Spectrom. 28 (1993) 1424.
[27] O. Vorm, P. Roepstorff, M. Mann, Anal. Chem. 66 (1994) 3281.
[28] S. Jespersen, V.M. Niessen, U.R. Tjaden, J. van der Greef, J. Mass. Spectrom. 33 (1998) 1088.
[29] R.C. Beavis, B.T. Chait, Rapid Commun. Mass Spectrom. 3 (1989) 436.
[30] C. Menzel, K. Dreisewerd, S. Berkenkamp, F. Hillenkamp, J. Am. Soc. Mass Spectrom. 13 (2002) 975.